articles

molecular pharmaceutics

Design of Potent Amorphous Drug Nanoparticles for Rapid Generation of Highly Supersaturated Media

Michal E. Matteucci,[†] Blair K. Brettmann,[†] True L. Rogers,[‡] Edmund J. Elder,[‡] Robert O. Williams, III,[§] and Keith P. Johnston*,[†]

Department of Chemical Engineering, The University of Texas, Austin, Texas 78712, College of Pharmacy, The University of Texas, Austin, Texas 78712, and The Dow Chemical Company, Midland, Michigan 48640

Received February 15, 2007; Revised Manuscript Received June 4, 2007; Accepted June 20, 2007

Abstract: Controlled precipitation produced aqueous nanoparticle suspensions of a poorly water soluble drug, itraconazole (ITZ), in an amorphous state, despite unusually high potencies (drug weight/total weight) of up to 94%. Adsorption of the amphiphilic stabilizer hydroxypropylmethylcellulose (HPMC) at the particle–aqueous solution interface arrested particle growth, producing surface areas from 13 to 51 m^2/g. Dissolution of the particles in acidic media yielded high plateau levels in supersaturation up to 90 times the equilibrium solubility. The degree of supersaturation increased with particle curvature, as characterized by the surface area and described qualitatively by the Kelvin equation. A thermodynamic analysis indicated HPMC maintained amorphous ITZ in the solid phase with a fugacity 90 times the crystalline value, while it did not influence the fugacity of ITZ in the aqueous phase. High surface areas led to more rapid and levels of supersaturation higher than those seen for low-surface area solid dispersions, which undergo crystallization during slow dissolution. The rapid generation of high levels of supersaturation with potent amorphous nanoparticles, containing small amounts of stabilizers oriented at the particle surface, offers new opportunities for improving bioavailability of poorly water soluble drugs.

Keywords: Supersaturation; amorphous pharmaceutical; nanoparticle dissolution; poorly water soluble drug; metastable solubility; itraconazole

1. Introduction

For biopharmaceutical classification system (BCS) type II drugs with high permeability through biomembranes, bioavailability in oral delivery is limited by the dissolution rate.[1–4] Particle size reduction of crystalline materials increases the surface area, A, while high-energy polymorphs, including the amorphous state, increase the solubility, C_{sat}, both leading to faster dissolution rates[4–10] as predicted by the Noyes–Whitney equation

$$\frac{dm}{dt} = \frac{DA}{h}(C_{sat} - C) \quad (1)$$

where D is the diffusion coefficient, h is the diffusional path length, and C is the concentration in solution. Precipitation of an organic drug solution with either water or a supercritical fluid antisolvent is commonly used to form high-surface area particles, both crystalline and amorphous. During precipitation, mixing energy[11–13] and stabilization with polymers are

* To whom correspondence should be addressed: Department of Chemical Engineering, The University of Texas, 1 University Station, C0400, Austin, TX 78712. Telephone: (512) 471-4671. Fax: (512) 475-7824. E-mail: kpj@che.utexas.edu.

[†] Department of Chemical Engineering, The University of Texas.

[‡] The Dow Chemical Co.

[§] College of Pharmacy, The University of Texas.

(1) Amidon, G. L.; Lennernas, H.; Sha, V. P.; Crison, J. R. A theoretical basis for a biopharmaceutic drug classification: The correlation of in vitro drug product dissolution and in vivo bioavailability. *Pharm. Res.* **1995**, *12*, 413–420.

(2) Horter, D.; Dressman, J. B. Influence of physicochemical properties on dissolution of drugs in the gastrointestinal tract. *Adv. Drug Delivery Rev.* **2001**, *46*, 75–87.

(3) Hancock, B. C.; Parks, M. What is the True Solubility Advantage for Amorphous Pharmaceuticals. *Pharm. Res.* **2000**, *17* (4), 397–404.

(4) Singhal, D.; Curatolo, W. Drug polymorphism and dosage form design: A practical perspective. *Adv. Drug Delivery Rev.* **2004**, *56*, 335–347.

10.1021/mp0700211 CCC: $37.00
Published on Web 08/24/2007

used to control particle size and morphology.[14–19] Therapeutic proteins are often formulated in the amorphous state with stabilizing excipients to ensure physical and chemical stability.[20,21] Theoretical solubilities of amorphous pharmaceuticals in aqueous media have been predicted with thermodynamic models to be 100-fold and up to 1600-fold greater than that of the crystalline form.[3,19,22] Experimentally measured solubilities, however, often reach only a fraction of the theoretical value, for example, 4.5 experimental versus ~100 theoretical for indomethacin.[3,19] A high degree of supersaturation for amorphous formulations will increase C_{sat} and thus the flux across biomembranes.[2,23–27] In this case, drug molecules are in a metastable state and may precipitate by nucleation and growth to lower the free energy. Particle growth of embryo crystals may be inhibited by coating drug particles with polymeric stabilizers,[25,28–31] particularly HPMC.[5,23,25,29]

Storage stability of an amorphous solid is a great concern, as the high-energy solid state may relax to the lower-free energy crystalline form. Properties such as the glass transition (T_g), reduced crystallization temperature ($T_c - T_g$ or $T_m - T_g$), and fragility of the amorphous drug can be used to describe the molecular mobility and characterize the stability at typical storage temperatures.[3,19,32–34] Solid dispersions and solid solutions with high-T_g polymers are often utilized to

(5) Yamashita, K.; Nakate, T.; Okimoto, K.; Ohike, A.; Tokunaga, Y.; Ibuki, R.; Higaki, K.; Kimura, T. Establishment of new preparation method for solid dispersion formulation of tacrolimus. *Int. J. Pharm.* **2003**, *267*, 79–91.

(6) Six, K.; Daems, T.; de Hoon, J.; Hecken, A. V.; Depre, M.; Bouche, M.-P.; Prinsen, P.; Verreck, G.; Peeters, J.; Brewster, M. E.; Van den Mooter, G. Clinical study of solid dispersions of itraconazole prepared by hot-stage extrusion. *Eur. J. Pharm. Biopharm.* **2005**, *24*, 179–186.

(7) Yamamoto, K.; Nakano, M.; Arita, T.; Takayama, Y.; Nakai, Y. Dissolution Behavior and Bioavailability of Phenytoin from a Ground Mixture with Microcrystalline Cellulose. *J. Pharm. Sci.* **1976**, *65* (10), 1484–1488.

(8) Fukuoka, E.; Makita, M.; Yamamura, S. Glass state of pharmaceuticals. 2: Bioinequivalence of glassy and crystalline indomethacin. *Chem. Pharm. Bull.* **1987**, *35*, 2943–2948.

(9) Lee, S.; Nam, K.; Kim, M. S.; Jun, S. W.; Park, J.-S.; Woo, J. S.; Hwang, S.-J. Preparation and Characterization of Solid Dispersions of Itraconazole by using Aerosol Solvent Extraction System for Improvement in Drug Solubility and Bioavailability. *Arch. Pharm. Res.* **2005**, *28* (7), 866–874.

(10) Kohri, N.; Yamayoshi, Y.; Xin, H.; Iseki, K.; Sato, N.; Todo, S.; Miyazaki, K. Improving the oral bioavailability of albendazole in rabbits by the solid dispersion technique. *J. Pharm. Pharmacol.* **1999**, *51* (2), 159–164.

(11) Jarmer, D. J.; Lengsfeld, C. S.; Randolph, T. W. Nucleation and Growth Rates of Poly(L-lactic acid) Microparticles during Precipitation with a Compressed-Fluid Antisolvent. *Langmuir* **2004**, *20*, 7254–7264.

(12) Chavez, F.; Debenedetti, P. G.; Luo, J. J.; Dave, R. N.; Pfeffer, R. Estimation of the Characteristic Time Scales in the Supercritical Antisolvent Process. *Ind. Eng. Chem. Res.* **2003**, *42*, 3156–3162.

(13) Johnson, B. K.; Prud'homme, R. K. Chemical Processing and Micromixing in Confined Impinging Jets. *AIChE J.* **2003**, *49* (9), 2264–2282.

(14) Rasenack, N.; Muller, B. W. Dissolution Rate Enhancement by in Situ Micronization of Poorly Water-Soluble Drugs. *Pharm. Res.* **2002**, *19* (12), 1894–1900.

(15) Horn, D.; Luddecke, E. Preparation and Characterization of Nanosized Carotenoid Hydrosols. *NATO Sci. Ser., 3* **1996**, *12*, 761–775.

(16) Rogers, T. L.; Gillespie, I. B.; Hitt, J. E.; Fransen, K. L.; Crowl, C. A.; Tucker, C. J.; Kupperblatt, G. B.; Becker, J. N.; Wilson, D. L.; Todd, C.; Broomall, C. F.; Evans, J. C.; Elder, E. J. Development and Characterization of a Scalable Controlled Precipitation Process to Enhance the Dissolution of Poorly Water-Soluble Drugs. *Pharm. Res.* **2004**, *21* (11), 2048–2057.

(17) Reverchon, E.; De Marco, I.; Caputo, G.; Della Porta, G. Pilot Scale Micronization of Amoxicillin by Supercritical Antisolvent Precipitation. *J. Supercrit. Fluids* **2003**, *26*, 1–7.

(18) Liu, Y.; Kathan, K.; Saad, W.; Prud'homme, R. K. Ostwald Ripening of β-Carotene Nanoparticles. *Phys. Rev.* **2007**, *98*, (3), 03102/1-036102/4.

(19) Gupta, P.; Chawla, G.; Bansal, A. K. Physical Stability and Solubility Advantage from Amorphous Celecoxib: The Role of Thermodynamic Quantities and Molecular Mobility. *Mol. Pharmaceutics* **2004**, *1* (6), 406–413.

(20) Roberts, C. J.; Debenedetti, P. G. Engineering Pharmaceutical Stability with Amorphous Solids. *AIChE J.* **2002**, *48* (6), 1140–1144.

(21) Lee, S. L.; Hafeman, A. E.; Debenedetti, P. G.; Pethica, B. A.; Moore, D. J. Solid-State Stabilization of α-Chymotrypsin and Catalase with Carbohydrates. *Ind. Eng. Chem. Res.* **2006**, *45*, 2134–5147.

(22) Parks, G. S.; Snyder, L. J.; Cattoir, F. R. Studies on Glass. XI. Some Thermodynamic Relations of Glassy and α-Crystalline Glucose. *J. Chem. Phys.* **1934**, *2*, 595–598.

(23) Raghavan, S. L.; Kiepfer, B.; Davis, A. F.; Kazarian, S. G.; Hadgraft, J. Membrane transport of hydrocortisone acetate from supersaturated solutions: The role of polymers. *Int. J. Pharm.* **2001**, *221* (1–2), 95–105.

(24) Hancock, B. C.; Zografi, G. Characteristics and significance of the amorphous state in pharmaceutical systems. *J. Pharm. Sci.* **1997**, *86*, 1–12.

(25) Kumprakob, U.; Kawakami, J.; Adachi, I. Permeation Enhancement of Ketoprofen Using a Supersaturated System with Antinucleant Polymers. *Biol. Pharm. Bull.* **2005**, *28* (9), 1684–1688.

(26) Jasti, B. R.; Berner, B.; Zhou, S.-L.; Li, X. A Novel Method for Determination of Drug Solubility in Polymeric Matrices. *J. Pharm. Sci.* **2004**, *93* (8), 2135–2141.

(27) Raghavan, S. L.; Trividic, A.; Davis, A. F.; Hadgraft, J. Effect of cellulose polymers on supersaturation and in vitro membrane transport of hydrocortisone acetate. *Int. J. Pharm.* **2000**, *193* (2), 231–237.

(28) Gao, P.; Rush, B. D.; Pfund, W. P.; Huang, T.; Bauer, J. M.; Morozowich, W.; Kuo, M.-s.; Hageman, M. J. Development of a supersaturable SEDDS (S-SEDDS) formulation of paclitaxel with improved oral bioavailability. *J. Pharm. Sci.* **2003**, *92* (12), 2386–2398.

(29) Gao, P.; Guyton, M. E.; Huang, T.; Bauer, J. M.; Stefanski, K. J.; Lu, Q. Enhanced Oral Bioavailability of a Poorly Water Soluble Drug PNU-91325 by Supersaturatable Formulations. *Drug Dev. Ind. Pharm.* **2004**, *30* (2), 221–229.

(30) Raghavan, S. L.; Trividic, A.; Davis, A. F.; Hadgraft, J. Crystallization of hydrocortisone acetate: Influence of polymers. *Int. J. Pharm.* **2001**, *212* (2), 213–221.

(31) Moser, K.; Kriwet, K.; Kalia, Y. N.; Guy, R. H. Stabilization of supersaturated solutions of a lipophilic drug for dermal delivery. *Int. J. Pharm.* **2001**, *224* (1–2), 169–176.

(32) Angell, C. A. Liquid Fragility and the Glass Transition in Water and Aqueous Solutions. *Chem. Rev.* **2002**, *102*, 2627–2650.

reduce the mobility of drug molecules, thereby preventing crystallization during both the particle formation step and storage.[5,35,36]

Amorphous drug formulations, either solid dispersions or co-ground mixtures with polymers such as HPMC,[5,36–41] poly(vinylpyrolidone),[42] polyethylene glycol,[43] aminoalkyl methacrylate copolymer (Eudragit E 100),[44] methacrylic acid-methacrylic acid methyl ester copolymer (Eudragit L),[45] carboxymethylethylcellulose,[45] and microcrystalline cellulose,[7] have been used to create supersaturated solutions. Suzuki et al. produced solid dispersions of nifedipine stabilized with HPMC and PVP at drug loadings (drug weight/total weight) from 11 to 33%, where supersaturation levels were up to 6 times the crystalline nifedipine solubility.[38,40] A supersaturation of 45 in 2 h was achieved in 0.1 N HCl for a solid dispersion of ITZ with HPMC formed by hot melt extrusion at a drug loading of 40%.[36,41] Amorphous solid dispersions of tacrolimus produced by solvent evaporation with PEG 6000, PVP, and HPMC at 50% drug loading were shown to supersaturate 0.1 N HCl up to 25 in 2 h.[5] In all of these studies, supersaturation levels were obtained only for drug loadings of ≤50%.

Previous studies of supersaturation from amorphous drug particles have focused primarily on solid dispersions with stabilizers dispersed throughout the entire particle.[5,36–45] These formulations had relatively low surface areas (<1 m^2/g) and required a large amount of stabilizer, typically 50% (weight) or more, to inhibit crystallization of drug domains and to achieve sufficient hydrophilicities on the particle surfaces for wetting. For high-dose drugs, it would be beneficial to produce amorphous particle formulations with larger drug loadings to achieve desired dosage sizes and to avoid side effects from excipients. The amount of amphiphilic stabilizer may be reduced by forming the particles in the presence of water to orient the stabilizer preferentially at the interface between the drug particle and aqueous solution. This approach has been utilized to form crystalline particles in antisolvent processes[16,46,47] and evaporative precipitation of organic[48–50] and supercritical fluid[51,52] solutions. Aqueous suspensions of sub-300 nm ITZ particles have been produced by CP with poloxamer 407 at drug loadings

(33) Angell, C. A. Thermodynamic Aspects of the Glass Transition in Liquids and Plastic Crystals. *Pure Appl. Chem.* **1991**, *63* (10), 1387–1392.
(34) Zhou, D.; Zhang, G. G. Z.; Law, D.; Grant, D. J. W.; Schmitt, E. A. Physical Stability of Amorphous Pharmaceuticals: Importance of Configurational Thermodynamic Quantities and Molecular Mobility. *J. Pharm. Sci.* **2002**, *91* (8), 1863–1872.
(35) Hasegawa, A.; Kawamura, R.; Nakagawa, H.; Sugimoto, I. Physical Properties of Solid Dispersions of Poorly Water-Soluble Drugs with Enteric Coating Agents. *Chem. Pharm. Bull.* **1985**, *33* (8), 3429–3435.
(36) Verreck, G.; Six, K.; Van den Mooter, G.; Baert, L.; Peeters, J.; Brewster, M. E. Characterization of solid dispersions of itraconazole and hydroxypropylmethylcellulose prepared by melt extrusion. Part I. *Int. J. Pharm.* **2003**, *251*, 165–174.
(37) Okimoto, K.; Miyake, M.; Ibuki, R.; Yasumura, M.; Ohnishi, N.; Nakai, T. Dissolution mechanism and rate of solid dispersion particles of nilvadipine with hydroxypropylmethylcellulose. *Int. J. Pharm.* **1997**, *159*, 85–93.
(38) Suzuki, H.; Sunada, H. Comparison of Nicotinamide, Ethylurea and Polyethylene Glycol as Carriers for Nifedipine Solid Dispersion Systems. *Chem. Pharm. Bull.* **1997**, *45* (10), 1688–1693.
(39) Suzuki, H.; Sunada, H. Influence of water-soluble polymers on the dissolution of nifedipine solid dispersions with combined carriers. *Chem. Pharm. Bull.* **1998**, *46* (3), 482–487.
(40) Suzuki, H.; Sunada, H. Some Factors Influencing the Dissolution of Solid Dispersions with Nicotinamide and Hydroxypropylmethylcellulose as Combined Carriers. *Chem. Pharm. Bull.* **1998**, *46* (6), 1015–1020.
(41) Six, K.; Berghmans, H.; Leuner, C.; Cressman, J.; Van Werde, K.; Mullens, J.; Benoist, L.; Thimon, M.; Meublat, L.; Verreck, G.; Peeters, J.; Brewster, M. E.; Van den Mooter, G. Characterization of Solid Dispersions of Itraconazole and Hydroxypropylmethylcellulose Prepared by Melt Extrusion. Part II. *Pharm. Res.* **2003**, *20* (7), 1047–1054.
(42) Yamada, T.; Saito, N.; Imai, T.; Otagiri, M. Effect of grinding with hydroxypropyl cellulose on the dissolution and particle size of a poorly water-soluble drug. *Chem. Pharm. Bull.* **1999**, *47* (9), 1311–1313.
(43) Urbanetz, N. A.; Lippold, B. C. Solid dispersions of nimodipine and polyethylene glycol 2000: Dissolution properties and physicochemical characterization. *Eur. J. Pharm. Biopharm.* **2005**, *59* (1), 107–118.
(44) Jung, J.-Y.; Yoo, S. D.; Lee, S.-H.; Kim, K.-H.; Yoon, D.-S.; Lee, K.-H. Enhanced solubility and dissolution rate of itraconazole by a solid dispersion technique. *Int. J. Pharm.* **1999**, *187*, 209–218.
(45) Hasegawa, A.; Taguchi, M.; Suzuki, R.; Miyata, T.; Nakagawa, H.; Sugimoto, I. Supersaturation Mechanism of Drugs from Solid Dispersions with Enteric Coating Agents. *Chem. Pharm. Bull.* **1988**, *36* (12), 4941–4950.
(46) Johnson, B. K.; Prud'homme, R. K. Engineering the direct precipitation of stabilized organic and block copolymer nanoparticles as unique composites. *Polym. Mater. Sci. Eng.* **2003**, *89*, 744–745.
(47) Horn, D.; Rieger, J. Organic Nanoparticles in the Aqueous Phase: Theory, Experiment, and Use. *Angew. Chem., Int. Ed.* **2001**, *40* (23), 4330–4361.
(48) Chen, X.; Benhayoune, Z.; Williams, R. O.; Johnston, K. P. Rapid dissolution of high potency itraconazole particles produced by evaporative precipitation into aqueous solution. *J. Drug Delivery Sci. Technol.* **2004**, *14* (4), 299–304.
(49) Sinswat, P.; Gao, X.; Yacaman, M.-J.; Williams, R. O., III; Johnston, K. P. Stabilizer Choice for Rapid Dissolving High Potency Itraconazole Particles Formed by Evaporative Precipitation Into Aqueous Solution. *Int. J. Pharm.* **2005**, *3.2* (1–2), 113–124.
(50) Vaughn, J. M.; Gao, X.; Yacaman, M.-J.; Johnston, K. P.; Williams, R. O. I. Comparison of powder produced by evaporative precipitation into aqueous solution (EPAS) and spray freezing into liquid (SFL) technologies using novel Z-contrast STEM and complimentary techniques. *Eur. J. Pharm. Biopharm.* **2005**, *60*, 81–89.
(51) Reverchon, E. Supercritical antisolvent precipitation of micro- and nano-particles. *J. Supercrit. Fluids* **1999**, *15* (1), 1–21.
(52) Young, T. J.; Mawson, S. M.; Johnston, K. P. Rapid Expansion from Supercritical to Aqueous Solution to Produce Submicron Suspensions of Water-Insoluble Drugs. *Biotechnol. Prog.* **2000**, *16* (3), 402–407.

up to 86%;[53] however, the morphology and dissolution behavior were not investigated. To date, supersaturation of dissolution media from amorphous nanoparticles of poorly water soluble drugs has not been reported for particles with high drug loadings.

The key objective of this study was to form amorphous ITZ nanoparticles with high drug loadings up to 80% to achieve unusually high supersaturation levels in acidic media. During particle formation, the orientation of the hydrophilic stabilizer HPMC near the surface of the particles may be expected to facilitate high drug loadings while still inhibiting particle growth and crystallization. In contrast, nearly all amorphous conventional solid dispersions, for example, ITZ and HPMC, are limited to 50% loading and surface areas of <2 m^2/g. The rapid dissolution of high-surface area nanoparticles has the potential to minimize the time window for solvent-mediated crystallization of the remaining solid phase and thereby favor higher supersaturation levels than for low-surface area solid dispersions.

Itraconazole was chosen as a model poorly water soluble drug, given its extremely high lyophilicity, that is, octanol/water partition coefficient (log P) of 5.66, as reported by Janssen Pharmaceutica. The particles were characterized by modulated differential scanning calorimetry and X-ray diffraction to determine the crystallinity, scanning electron microscopy, Z-contrast transmission electron microscopy, X-ray photoelectron spectroscopy, BET surface area analysis, and contact angle measurements. The supersaturation behavior of aqueous suspensions and dry powders containing ITZ was investigated in 0.1 N HCl acidic media. Contact angles with 0.1 N HCl were compared for the CP powders relative to solid dispersions formed by solvent evaporation to demonstrate preferential orientation of HPMC on the particle surface for the CP powders.

The ITZ/HPMC suspensions were added to the dissolution media in increments to determine the maximum supersaturation level, which will be shown to approach the metastable solubility limit. High supersaturation values are facilitated by trapping ITZ in the amorphous state even for high drug loading. To place these results in perspective, the metastable solubility of a pure amorphous ITZ suspension was measured without any HPMC. A thermodynamic scheme was developed to examine the effect of HPMC on the fugacity of ITZ in the solid phase relative to the aqueous phase and to determine the ratio of amorphous and crystalline ITZ fugacity. The HPMC concentration influences the particle surface area during controlled precipitation and thus the supersaturation as predicted by the Kelvin equation. Mass transfer models were developed in an attempt to understand how the surface area and erosion of slowly dissolving HPMC influenced the dissolution rate. The exceptionally high surface area of the aggregated nanoparticles, with high wetted hydrophilic surface areas, will be shown to produce more rapid and higher levels of supersaturation than in the case of lower-surface area solid dispersions (SD) with less hydrophilic surfaces.

(53) Matteucci, M. E.; Hotze, M. A.; Williams, R. O. I.; Johnston, K. P. Drug Nanoparticles by Antisolvent Precipitation: Mixing Energy Versus Surfactant Stabilization. *Langmuir* **2006**, *22* (21), 8951–8959.

2. Materials and Methods

2.1. Materials. BP grade ITZ was purchased from Hawkins, Inc. (Minneapolis, MN). HPMC E5 (viscosity of 5 cP in a 2% aqueous 25 °C solution) grade was a gift from The Dow Chemical Co. Poly(vinylpyrolidone) K15 (PVPK15) and poloxamer 407 (P407) NF grade were both obtained from Spectrum Chemical (Gardena, CA). Stabilized pa grade 1,3-dioxolane was purchased from Acros Organics (Morris Plains, NJ). HPLC grade acetonitrile (ACN), ACS grade hydrochloric acid (HCl), and diethanolamine (DEA) were used as received from Fisher Chemicals (Fairlawn, NJ).

2.2. Controlled Precipitation into Aqueous Solution. The method of CP developed by Rogers et al.[16] was used to produce nanoparticle suspensions of itraconazole. Deionized water (120 g) containing an appropriate quantity of HPMC was used as the antisolvent phase into which 30 g of 1,3-dioxolane containing 3.3% (weight) ITZ was injected to form a fine precipitate. The organic phase was separated from the aqueous suspension via vacuum distillation. In some cases, the aqueous suspension was added dropwise to liquid nitrogen and lyophilized to form a powder using a Virtis Advantage Tray Lyophilizer (Virtis Co., Gardiner, NY) with primary drying at −35 °C for 24 h followed by secondary drying at 25 °C for 36 h. Dried powders were stored in a 13% relative humidity environment.

2.3. Solvent Evaporation To Form a Solid Dispersion (SD). Approximately 2 g of ITZ was added to 20 mL of dichloromethane and the mixture agitated until the ITZ was completely dissolved. The ITZ solution was placed in a mortar, and an appropriate amount of HPMC was slowly added while the mixture was gently stirred with a pestle without any precipitation. The solution was stirred gently until approximately 90% of the dichloromethane volume was evaporated, leaving a clear viscous gel. The remaining dichloromethane was removed by heating to 50 °C at a reduced pressure of ∼500 mtorr for 2 h. The resulting drug/polymer film was removed from the mortar and pestle with a straight razor blade and ground to a fine powder for 30 min using a ceramic ball mill (1 cm bead size). The final powder was collected after filtration through a size 16 mesh sieve (<1190 μm pore size).

2.4. Solubility Determination. To determine the solubility of crystalline ITZ at 37.2 °C, approximately 1.5 mg of bulk ITZ was placed in a glass vials containing 100 mL of 0.1 N HCl (pH 1.2). Two aliquots were removed from each vial after 18 h, immediately filtered with a 0.2 μm syringe filter, and diluted by one-half with ACN. Similarly, solubility was determined for solutions containing HPMC. Approximately 50 mg of ITZ was added to 100 mL of HPMC dissolved in 0.1 N HCl at concentrations of 0.5, 1, and 3.4 mg/mL. In all cases, drug concentrations were determined by high-performance liquid chromatography as described below with an n of at least 3.

2.5. Supersaturation Dissolution. Metastable solubility limits and rates of supersaturation were measured in 0.1 N HCl (pH 1.2) at 37.2 °C. A USP paddle method was adapted to accommodate smaller sample sizes using a VanKel VK6010 Dissolution Tester with a Vanderkamp VK650A heater/circulator (VanKel, Cary, NC). Dissolution media (50 mL) were preheated in small 100 mL capacity dissolution vessels (Varian Inc., Cary, NC). Suspensions were added dropwise to the dissolution media at a rate of approximately 10 drops/min to reduce the amount of excess particle dosing after the solubility limit had been reached. The drops were no longer added when particles could barely be detected by the naked eye, minimizing heterogeneous sites for nucleation of the supersaturated solutions. In the case of powder dissolution, a sample weight (~17.6 mg of drug) equivalent to approximately 80 times the equilibrium solubility (4.4 μg/mL, from the solubility study) of ITZ in 0.1 N HCl was added to the media. Sample aliquots (1.5 mL) were taken at various time points. The aliquots were filtered immediately using a 0.2 μm syringe filter, and 0.8 mL of the filtrate was subsequently diluted with 0.8 mL of ACN. To investigate the possibility of sub-200 nm particles passing through the 0.2 μm filter, the experiment was also conducted using a 0.02 μm syringe filter. In all cases, the filtrate was completely clear upon visual inspection, and dynamic light scattering of the filtrate gave a count rate of less than 20K cps (too small for particle size analysis). For all samples, the drug concentration was quantified by high-performance liquid chromatography as described below.

2.6. High-Performance Liquid Chromatography (HPLC). ITZ concentrations were quantified using a Shimadzu (Columbia, MD) LC-600 HPLC system. The mobile phase consisted of ACN, water, and DEA (70:30:0.05), and the flow rate was 1 mL/min. Using a detection wavelength of 263 nm, the ITZ peak eluted at 5.4 min. The standard curve linearity was verified from 500 to 1 μg/mL with an r^2 value of at least 0.999.

2.7. Scanning Electron Microscopy (SEM). Aqueous suspensions were diluted by one-tenth using pure deionized water and then flash-frozen onto aluminum SEM stages. After lyophilization to remove all water, the remaining particles were gold-palladium sputter coated for 35 s. Micrographs were taken using a Hitachi S-4500 field emission scanning electron microscope with an accelerating voltage of 10 kV.

2.8. X-ray Diffraction (XRD). Wide-angle X-ray scattering was employed to detect the crystallinity of dried drug powders using Cu $K\alpha_1$ radiation with a wavelength of 1.54054 Å at 40 kV and 20 mA from a Philips PW 1720 X-ray generator (Philips Analytical Inc., Natick, MA). A small amount of powder was pressed onto a glass slide to form a flat sample surface. The reflected intensity was measured at a 2θ angle between 10 and 30° with a step size of 0.05° and a dwell time of 9 s.

2.9. Temperature-Modulated Differential Scanning Calorimetry (mDSC). Drug crystallinity was detected by a model 2920 modulated differential scanning calorimeter (TA Instruments, New Castle, DE) with a refrigerated cooling system. The samples were purged with nitrogen at a flow rate of 150 mL/min. Samples were scanned after being placed in hermetically sealed aluminum pans. The amplitude used was 1 °C, the period 1 min, and the underlying heating rate 5 °C/min. Integration of the area under the ITZ melting endotherm at 168 °C and crystallization peak at approximately 120 °C estimated the percent crystallinity in the original sample (prior to DSC heating) by

$$x_{\text{cryst}} = \frac{\Delta h_{\text{melt}} - \Delta h_{\text{cryst}}}{\Delta h_{\text{meltItz}}} \quad (2)$$

where x_{cryst} is the percent crystallinity, Δh_{melt} is the heat of melting, Δh_{cryst} is the heat of crystallization, and $\Delta h_{\text{meltItz}}$ is the heat of melting for pure crystalline ITZ. It was assumed that the heat necessary to melt 1 g of crystalline ITZ and that necessary to crystallize 1 g of amorphous ITZ are equal. For a purely crystalline material, the melting peak area will be equal to that of the bulk material and no crystallization peak will be observed, giving a value of 1 for x_{cryst}. For a completely amorphous material, either no melting or crystallization peak will be observed or any crystallization peak area will be equal to the melting peak area, both giving an x_{cryst} value of 0.

2.10. BET Surface Area Measurement. Powder specific surface areas for approximately 0.05–0.2 g of drug powder were measured using a Quantichrome Instruments (Boynton Beach, FL) Nova 2000 series surface area analyzer using nitrogen as the adsorbate gas. Six points were taken over a range of relative pressures from 0.05 to 0.35. In all cases, correlation coefficients were greater than 0.99, indicating good linear fit with the Brunauer–Emmett–Teller (BET) equation.

2.11. Contact Angle Measurement. A 50 mg quantity of drug powder was compacted into a tablet using a model M Carver laboratory press (Fred S. Carver, Inc., Menomonee Falls, WI) with a compression force of 500 kg. The contact angle between the compressed powder and a 0.03 mL drop of 0.1 N HCl was measured using a model 100-00-115 goniometer (Rame-Hart Inc., Mountain Lakes, NJ).

3. Results and Discussion

3.1. High-Potency Amorphous Nanoparticle Suspensions Made by Controlled Precipitation. Aqueous nanosuspensions of ITZ with a range of drug:stabilizer ratios from 4:1 to 1:2 were formed by CP and characterized by a variety of techniques. As listed in Table 1, BET surface areas of powders formed by freeze-drying the nanosuspensions ranged from ~13 to 51 m^2/g. Spherical particles approximately 200–600 nm in diameter were observed in the scanning electron micrographs shown in Figure 1 A–D, as well as fibrous morphologies with diameters of less than 50 nm. Primary particle domains on the order of 50–100 nm were detected by Z-contrast STEM, shown in Figure 1 G,H. As the stabilizer concentration increased, the surface area increased, with a corresponding decrease in average particle size. Much larger morphologies and surface areas were observed for

Table 1. Specific Surface Area of Dried Powders Produced by CP and Solvent Evaporation (SD)

formulation	BET area (m^2/g)	formulation	BET area (m^2/g)
1:2 ITZ/HPMC	51	4:1 ITZ/HPMC SD	<2
1:1 ITZ/HPMC	23	1:1 ITZ/HPMC SD	<2
2:1 ITZ/HPMC	17	16:1 ITZ/HPMC SD	<2
4:1 ITZ/HPMC	13		

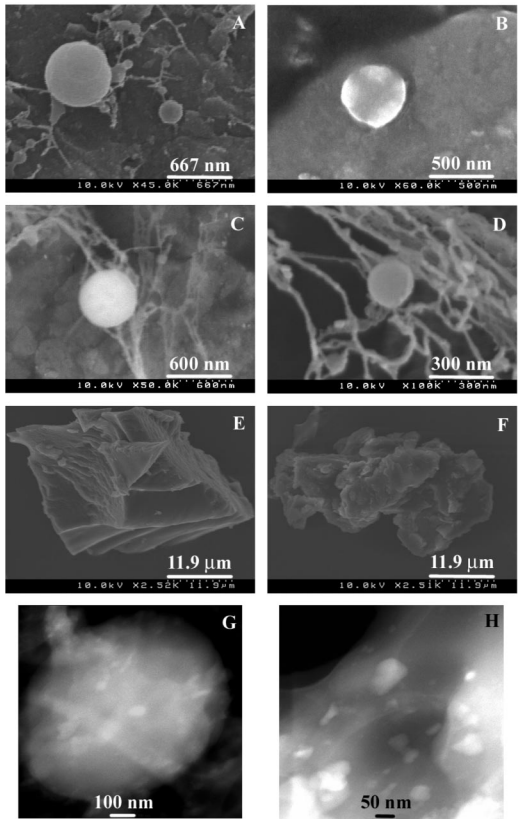

Figure 1. SEM (A–F) and Z-Contrast STEM (G and H) images of dried controlled precipitation powders (A–D, G, and H) and solid dispersions (E and F): (A) 4:1, (B) 2:1, (C) 1:1, (D) 1:2, (E) 4:1, (F) 16:1, and (G and H) 1:2 ITZ/HPMC.

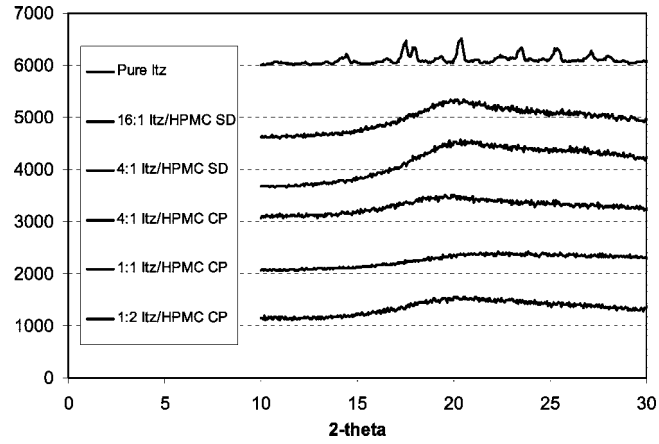

Figure 2. X-ray diffraction (XRD) of CP dry powders and solid dispersions.

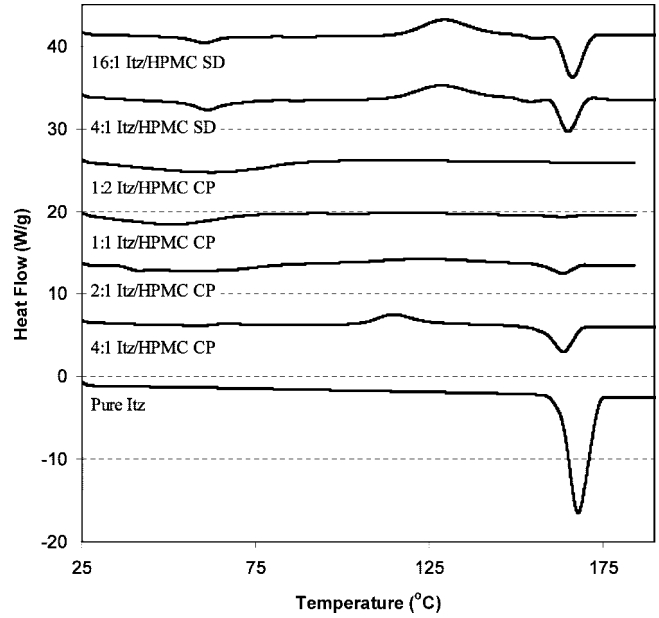

Figure 3. Modulated differential scanning calorimetry (mDSC) of CP powders with drug loading from 33 to 80% and pure ITZ.

the SD powders in Figure 1 E,F. From XRD, characteristic peaks of crystalline ITZ were not detected for any of the samples (Figure 2). For these amorphous submicrometer particles, the crystalline content was below the detection limit of XRD.[54,55] From further evaluation by mDSC (Figure 3 and Table 2) at low stabilizer concentrations (4:1 and 2:1 ITZ/HPMC), both a melting peak and a crystallization peak were observed. The crystallization peak resulted from the transformation of amorphous ITZ to its stable crystalline form upon heating.[56–58] The endotherm observed at 168 °C was caused by melting of both drug crystals formed in situ as well as those which were present in the original sample, prior to DSC heating. At high drug loadings (4:1 and 2:1 ITZ/HPMC), the presence of a crystallization and melting peak suggested up to 24% crystallinity present in the original sample. At higher stabilizer concentrations (1:1 and 1:2 ITZ/HPMC), a crystallization peak was not present and the melting endotherm was small or nonexistent, indicating highly amorphous material. SD powders exhibited both a crystallization and melting peak with similar areas; therefore, they were estimated as being purely amorphous. As also shown in Table 2, the contact angle for the SD powders with 0.1 N HCl (75 ± 2°) was comparable to that of the bulk drug with no stabilizer (72 ± 0.75°). For CP powders, the lower contact angle of 53 ± 2° approached that of

(54) Saleki-Gerhardt, A.; Ahlneck, C.; Zografi, G. Assessment of disorder in crystalline solids. *Int. J. Pharm.* **1994**, *101* (3), 237–247.

(55) Buckton, G.; Darcy, P. Assessment of disorder in crystalline powders: A review of analytical techniques and their application. *Int. J. Pharm.* **1999**, *179* (2), 141–158.

Table 2. Contact Angles of Dried Powders with 0.1 N HCl, Heats of Melting and Crystallization Measured by mDSC, and Estimated Percent Crystallinities [$y = (\Delta h_{fus} - \Delta h_{cryst})/\Delta h_{fusITZ}$]

sample	predicted contact angle (θ_c, from eq *3*)	contact angle (θ)	Δh_{cryst}/potency (J/g)	Δh_{fus}/potency (J/g)	$\Delta h_{fus} - \Delta h_{cryst}/\Delta h_{fusITZ}$
4:1 ITZ/HPMC CP	68.9	53.2±2.10	40.3	60.8	0.24
2:1 ITZ/HPMC CP	–	–	15.0	26.5	0.14
1:1 ITZ/HPMC CP	64.2	61.1±1.76	0	6.80	0.08
1:2 ITZ/HPMC CP	–	–	0	0	0
4:1 ITZ/HPMC SD	68.9	74.9±2.20	14.1	16.3	0.03
1:1 ITZ/HPMC SD	64.2	74.9±2.70	–	–	–
16:1 ITZ/HPMC SD	–	–	34.9	33.3	–0.02
pure HPMC	–	55.8±1.62	0	0	0
pure ITZ	–	72.0±0.75	0	84.7	1.0

Table 3. X-ray Photoelectron Spectroscopy (XPS) of 4:1 ITZ/HPMC Dried Powders Made by CP and Solvent Evaporation (SD)

sample	area of nitrogen peak (at ~400 eV)	% surface of ITZ	% surface excess of ITZ	% relative surface excess[a] of ITZ	% relative surface excess[a] of ITZ from contact angle
pure ITZ	2875	–	–	–	–
4:1 ITZ/HPMC CP	1353	47	−33	−41	−23
4:1 ITZ/HPMC SD	2814	98	18	22	8.7

[a] The % relative surface excess of ITZ = 100(actual – predicted)/predicted, where the predicted value is for random mixing.

bulk HPMC (56 ± 2°) and indicated a much more hydrophilic surface.

Surface composition analysis by X-ray photoelectron spectroscopy (XPS) was used to approximate the surface nitrogen content of dried powders, from integration of the peak at ~400 eV (Table 3), as done previously for other drugs.[59,60] Whereas ITZ contains eight N atoms, HPMC does not contain any N. For pure ITZ, the integrated area was 2875, as shown in Table 3. A 4:1 ITZ/HPMC CP powder gave an area of 1353, indicating approximately 47% (1353/2875) ITZ on the surface. For the 4:1 ITZ/HPMC SD, a peak area of 2814 corresponded to 98% (2814/2875) surface ITZ. For both powders, the predicted surface concentration of ITZ was 80% for random mixing in the 4:1 ITZ/HPMC formulation. For the CP mixture, the surface excess was 47 – 80 = −33% and the relative surface excess was −33/80 = −41%, indicating preferential orientation of the HPMC on the surface.

Additionally, contact angle measurements (Table 2) may be used to determine the surface excess. For random mixing of ITZ and HPMC,[61] the predicted value of

$$\cos \theta_c = f_1 \cos \theta_1 + f_2 \cos \theta_2 \qquad (3)$$

According to the experimental contact angle and eq 3, the % relative surface excesses of ITZ were −23% for 4:1 ITZ/HPMC CP and 8.7% for 4:1 ITZ/HPMC SD. Although these values were each smaller in magnitude than that for the relative surface excess from XPS, the signs were the same. In addition, the magnitude was greater for the CP formulation than for the SD formulation in each method. The smaller magnitudes (closer to random mixing) for the contact angles may indicate that they probe more deeply into the surface of the solid. In addition, the contact angle measurements are influenced by hydrogen bonding between water and hydroxyl groups in the HPMC, a factor not present for the XPS data.

When the organic and aqueous solutions were mixed in CP, rapid nucleation produces a large interfacial area between the hydrophobic ITZ particle surface and the surrounding aqueous solution. For 1–100 nm growing drug particles, interfacial areas from 6000 to 60 m^2/g provide a strong driving force for adsorption of the amphiphilic stabilizer, HPMC, to lower the interfacial energy. Given the strong polar and hydrogen bonding interactions of HPMC with water, the

(56) Hohne, G. W. H.; Hemminger, W. F.; Flammersheim, H.-J. *Differential Scanning Calorimetry*, 2nd ed.; Springer: New York, 2003.

(57) Sertsou, G.; Butler, J.; Hempenstall, J.; Rades, T. Solvent change co-precipitation with hydroxylpropyl methylcellulose phthalate to improve dissolution characteristics of a poorly water-soluble drug. *J. Pharm. Pharmacol.* **2002**, *54*, 1041–1047.

(58) Inoue, K.; Ogawa, K.; Okada, J. i.; Sugibayashi, K. Enhancement of skin permeation of ketotifen by supersaturation generated by amorphous form of the drug. *J. Controlled Release* **2005**, *108*, 306–318.

(59) Yu, Z.; Johnston, K. P.; Williams, R. O. I. Spray freezing into liquid versus spray-freeze drying: Influence of atomization on protein aggregation and biological activity. *Eur. J. Pharm. Biopharm.* **2006**, *27*, 9–18.

(60) Webb, S. D.; Golledge, S. L.; Cleland, J. L.; Carpenter, J. F. Surface Adsorption of Recombinant Human Interferon-γ in Lyophilized and Spray-Lyophilized Formulations. *J. Pharm. Sci.* **2002**, *91* (6), 1474–1487.

(61) Adamson, A. W. *Physical Chemistry of Surfaces*, 6th ed.; John Wiley & Sons: New York, 1997.

tendency of HPMC to precipitate within the hydrophobic interior of the ITZ particles is relatively weak. Instead, the interfacial activity orients the polymer on the surface of the drug particle. Additional HPMC in the aqueous phase will coat the particles upon drying. In the case of solvent evaporation, the precipitating drug and polymer are exposed to a solvent–air interface. The drug has a lower cohesive energy density than HPMC and will have a stronger tendency to partition to this interface, creating a particle surface which is rich in drug, as observed.

The ratio of the mixing time of the solvent and antisolvent relative to the precipitation time is described by the dimensionless Damkohler number, Da.[46,53] As shown for ITZ, increasing the stabilizer concentration increases the time for growth by coagulation and decreases Da, reducing the particle size to 300 nm.[53] As the stabilizer adsorbs to the growing particle surface, it may impede incorporation of drug molecules into a crystalline lattice structure and slow the crystallization rate. A high concentration is available to arrest growth on the surface, even for high drug loadings. The high level of supersaturation in CP and the rapid removal of the growing particles from the mixing zone appear to produce rapid nucleation and slow growth of amorphous ITZ particles without crystallization as shown in the mDSC and X-ray diffraction data. For the case of SD powders made by hot melt extrusion, slow precipitation at high drug loadings led to significant growth, crystallization,[41] and low surface areas. For up to 3:2 ITZ/HPMC, a solid solution was formed, but for higher loadings of ITZ, phase separation was observed.[41] Whereas the method of CP has been used to precipitate submicrometer-sized crystalline particles of several drugs, including naproxen, danazol, and ketoconazole,[16] this method led to amorphous ITZ in the current study.

3.2. Supersaturation of Aqueous Media with a Stabilizer-Free Drug Suspension. The simplest formulation was studied first, a suspension of pure amorphous ITZ with no stabilizer present. Without stabilizer present to prevent growth, the average particle size was approximately 10 μm, according to laser light scattering measurement. The suspension was added dropwise to 0.1 N HCl medium until no further dissolution was observed visually. As shown in Figure 4, the drug concentration reached 277 μg/mL in 4 h, 63 times the equilibrium solubility of crystalline ITZ, which was 4.4 μg/mL. The supersaturation reached a plateau up to 4 h without precipitating; therefore, it is reasonable to define this condition as a metastable equilibrium state for the amorphous drug particles.

The theoretical mole fraction of dissolved drug, component 2, in a liquid phase is

$$x^{L}_{2} = \frac{f_{2(\text{solid})}}{\gamma_2 f_{2(\text{solid})}} \tag{4}$$

where $f_{2(\text{solid})}$ is the fugacity of the pure solid drug, f_2^{0L} is the standard-state fugacity of the pure hypothetical subcooled liquid drug, and γ_2 is the activity coefficient in the liquid

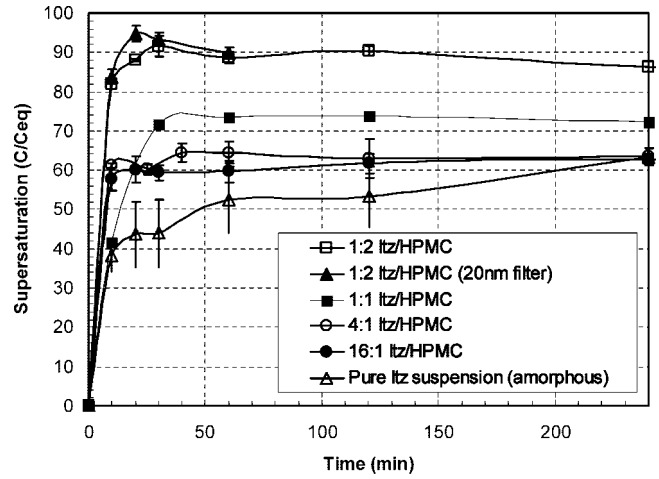

Figure 4. Maximum supersaturation levels of CP nanoparticle suspensions after dropwise addition to 0.1 N HCl medium (all samples were filtered with a 0.2 μm filter unless noted otherwise). Suspensions (~10 mg of ITZ/mL) were added until undissolved particles were barely detected, indicating the solubility limit (50 mL of 0.1 N HCl, 37.2 °C, paddle speed of 50 rpm).

phase.[62] The well-known fugacity ratio for a pure crystalline material is given by[62]

$$\ln\left[\frac{f_2}{f_{2(\text{solid})}}\right] = \frac{\text{MW}_{\text{Itz}}\Delta h_{\text{meltItz}}}{\text{RT}_{\text{m}}}\left(\frac{T_{\text{m}}}{T} - 1\right) \tag{5}$$

where T_{m} is 399 K, T is 310 K, $\Delta h_{\text{meltItz}}$ is 84.7 J/g, and MW_{Itz} is 705 g/mol. The difference in heat capacity in the solid and liquid phases is small and was assumed to be zero. On the basis of the crystalline solubility of 4.4 μg/mL ($x^{L}_{2} = 1.12 \times 10^{-7}$), eq 4 gives a γ_2 of 9350. For amorphous ITZ with a supersaturation of 63, x^{L}_{2} is still only 7×10^{-6} and γ_2 changes less than 0.1%, on the basis of a simple two-suffix Margules equation.[62] Since γ_2 is essentially constant, $f_{2(\text{solid})}$ for amorphous ITZ is approximately 63 times greater than that of crystalline ITZ. In essence, the supersaturation directly determines the increase in $f_{2(\text{solid})}$ of pure ITZ.

In a control experiment, pure crystalline ITZ was added to a 3.4 mg/mL HPMC solution in 0.1 N HCl. The equilibrium solubility was 5.7 ± 0.06 μg/mL, not far above the value without HPMC of 4.4 μg/mL. Thus, the molecular interactions between ITZ and HPMC in solution had a modest effect on γ_2, despite a concentration of HPMC more than 500-fold greater than that of ITZ.

When the amorphous ITZ suspension was added to an acidic HCl aqueous solution also containing 3.4 mg/mL HPMC, the maximum supersaturation of 68 at 4 h was similar to that observed without any HPMC. All supersaturation values were reported relative to 4.4 μg/mL ITZ to maintain consistency, even when HPMC was present. Again, the intermolecular interactions between ITZ and HPMC in solution did not influence γ_2 as was seen above for crystalline ITZ. At 4 h, the supersaturation

(62) Prausnitz, J. M.; Lichtenthaler, R. N.; Azevedo, E. G. *Molecular Thermodynamics of Fluid-Phase Equilibria*, 3rd ed.; Prentice Hall: Upper Saddle River, NJ, 1999.

Table 4. Supersaturation at 4 and 24 h for Nanoparticle Suspensions with and without Additional HPMC Added to the Dissolution Medium (under the conditions used for Figure *4*)

sample	*S* at 4 h	C_{ITZ} at 4 h (μg/mL)	C_{HPMC} at 4 h (μg/mL)	*S* at 24 h
1:0 ITZ/HPMC	63 ± 9.7	280	0	28 ± 16
16:1 ITZ/HPMC	63 ± 0.8	280	17	50 ± 1.5
4:1 ITZ/HPMC	63 ± 2.1	280	69	61 ± 1.1
16:1 ITZ/HPMC with HPMC in medium (3.4 mg/mL)	63 ± 0.8	280	3400	60 ± 0.8
1:0 ITZ/HPMC with HPMC in medium (3.4 mg/mL)	68 ± 4.1	300	3400	68 ± 4.5

depended upon the amorphous state of the pure solid and was independent of the HPMC dissolved in the acidic HCl aqueous solution. For ITZ/HPMC systems in this study, the primary role of polymer is shown to be stabilization of high-surface area amorphous particles during the formation of the particles. Unlike previous supersaturation studies with HPMC, we demonstrated that the HPMC in the dissolution medium does not influence the initial level of supersaturation, for example, over the first 4 h. However, in some cases, much larger amounts of stabilizers and/or cosolvents have been used to enhance solubility when high drug loading is not a requirement in the dosage form[63] (i.e., Sandimmun Neoral).

3.3. Surface Area and Maximum Supersaturation of CP Nanoparticle Suspensions for Various Drug Loadings. Supersaturation in 0.1 N HCl medium was studied as a function of drug loading in the nanoparticle suspensions. As shown in Figure 4 and Table 4 for 94 and 80% drug loadings (16:1 and 4:1 ITZ/HPMC), the maximum supersaturation level was 63, similar to that of the pure drug suspension without HPMC. The supersaturated solutions were stable against precipitation for up to at least 4 h in all cases. As will be discussed in the next section, the nucleation and growth of the supersaturated ITZ solution were very slow for 4:1 ITZ/HPMC over 24 h. Thus, the plateau for the supersaturation in Figure 4 may be considered to be in metastable equilibrium between the slight excess of amorphous particles and the dissolved drug.

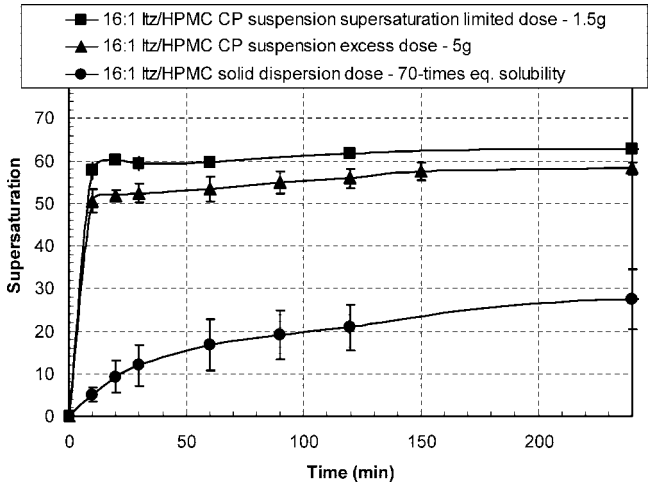

Figure 5. Supersaturation of a 16:1 ITZ/HPMC CP nanoparticle suspension at maximum supersaturation-limited dose and excess dose compared with a solid dispersion dose of 70 times equilibrium (under the conditions used for Figure 4). See the text for a description of dosing.

At a much lower drug loading of 33% (1:2 ITZ/HPMC), the supersaturation level reached ~90, 50% higher than for 4:1 ITZ/HPMC and pure ITZ. To make sure that undissolved particles did not pass through the 0.2 μm filter, the experiment was repeated with the 20 nm filter, and the supersaturation levels were unchanged. If all of the HPMC were to dissolve, the HPMC concentration in solution would be 0.79 mg/mL. This concentration is much lower than the case of 3.4 mg/mL in the two control experiments described above for both pure amorphous and pure crystalline ITZ, where the ITZ solubility and γ_2 changed relatively little with HPMC. For the current amorphous ITZ/HPMC suspensions, the effect of molecular interactions between ITZ and HPMC in the aqueous solution on γ_2 must be very minor. Therefore, the fugacity ratio of amorphous ITZ in the ITZ/HPMC particles to crystalline ITZ may again be equated to the supersaturation.

In another control experiment, a large excess amount of the 16:1 ITZ/HPMC suspension, 5 g, was added to the dissolution medium, as shown in Figure 5. The maximum supersaturation level was similar to the case where only 1.5 g of suspension was added to produce only a slight excess of undissolved particles. Thus, the excess suspended particles did not appear to nucleate the drug from the supersaturated solution over 4 h. Both cases may be considered to be at approximately the same metastable equilibrium saturation value, again supporting the argument that additional HPMC in solution has little effect on γ_2. The 5 g dose of suspension provided a HPMC concentration of approximately 55 μg/mL, still far lower than the HPMC concentration of 3.4 mg/mL added for the control experiments in Table 4. Furthermore, the similarity in the curves helps validate the hypothesis of the experimental procedure that the onset of turbidity with added suspension indicates the limit of supersaturation.

The relative solubility of two particles with different radii may be determined from the Kelvin equation[61] as follows:

$$\frac{x_a}{x_b} = \exp\left[\frac{2\gamma V_m}{RT}\left(\frac{1}{r_a} - \frac{1}{r_b}\right)\right] \quad (6)$$

where x is the solubility of a dissolved solid, γ is the interfacial tension between the particle and the solvent, V_m is the molar volume of the solute, and r is the particle radius. On the basis of the experiments described above, the activity coefficient of the solute in solution is essentially the same in each case. The increase in surface area from higher

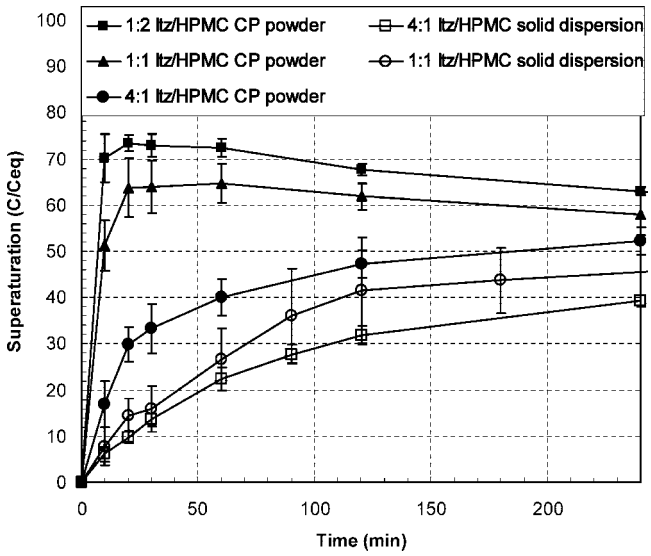

Figure 6. Supersaturation of CP dry powders and solid dispersions with drug loading from 33 to 80% at a constant dose of 80 times the equilibrium concentration (under the conditions used for Figure 4).

stabilizer concentrations indicates particles with smaller radii of curvature. This small curvature can come from either spherical or fibrous particle morphologies, as both were seen in SEMs. For example, according to the Kelvin equation and assuming $\gamma = 50$ mN/m (based on saturated hydrocarbon chains, for example, dodecane, with water),[64] an increase in the level of supersaturation from 63 to 90 would correspond to a diameter decrease from ~500 to 100 nm. This change in diameters is consistent with the change in surface areas for these two samples. Thus, the higher plateau levels in supersaturation as a function of the radii of curvature, for particles and fibers, as characterized by both the SEMs and BET surface area, are in qualitative agreement with the Kelvin equation.

3.4. Growth Inhibition by HPMC Adsorption. The most rapid precipitation from the supersaturated solutions was observed for the pure drug suspension without any HPMC. As shown in Table 4, the supersaturation decreased from 63 to 28 between 4 and 24 h. Precipitation rates were slower for 16:1 ITZ/HPMC, and negligible for 4:1 ITZ/HPMC. When additional HPMC was dissolved in the dissolution medium at a concentration of 3.4 mg/mL, precipitation of both pure drug and the 16:1 ITZ/HPMC suspension was completely inhibited, without any depletion in supersaturation over 24 h. However, the additional HPMC did not change the maximum supersaturation levels at shorter times.

Precipitation from the supersaturated solutions may be examined in terms of nucleation and growth rates. Amphiphilic polymers such as HPMC lower the interfacial energy (γ) between a hydrophobic embryo and aqueous media. The rate of homogeneous nucleation is defined[65]

$$B_o = C \exp\left\{\frac{-16\pi\gamma^3 V_m N_A}{3(RT)^3[\ln(S)]^2}\right\} \quad (7)$$

where C is the frequency factor, N_A is Avogadro's number, and the supersaturation $S = x^L{}_2$/(crystalline solubility). When $S = 60$, when γ is lowered from 20 to 10 mJ/m^2, B_o increases by many orders of magnitude, from 10^{-36} to 10^{16}, as observed for other systems.[61] For the case of a pure drug suspension without HPMC, γ is highest and B_o is lowest. However, precipitation was the fastest for the pure drug suspension. Therefore, the increase in the stability of the supersaturated solutions with HPMC in the particle formulations, or added to the medium, despite an increase in B_o must be caused by a decrease in growth rates.

The growth takes place by condensation (addition of drug molecules to growing particles) and by coagulation of particles. Growth was most rapid for the pure particles without any HPMC. In the case of 4:1 ITZ/HPMC, there was sufficient HPMC in the particle formulation itself to fully inhibit growth for 24 h, but not for 16:1 ITZ/HPMC. However, for 16:1 ITZ/HPMC, the preaddition of dissolved HPMC to the medium maintained a supersaturation level of 60 over the entire 24 h period, indicating the dissolved polymer was able to diffuse and adsorb to the drug particle surfaces. The adsorption of a polymer such as HPMC onto the surface of a growing particle may inhibit incorporation of drug molecules onto active sites for particle growth. Furthermore, loops and dangling ends of HPMC adsorbed on the surface may provide steric stabilization to retard coagulation.[66]

3.5. Effects of Surface Area on the Rate of Supersaturation for Freeze-Dried CP Nanoparticles and Microparticles Produced by Solvent Evaporation. Figure 6 compares the supersaturation profiles of several CP dried powders with a range of surface areas (listed in Table 5) as well as those of two low-surface area SD powders produced by solvent evaporation. As the particle surface area increased, supersaturation rates of the dried powders increased and the maximum levels were higher. For example, at a drug loading of 4:1 ITZ/HPMC, the CP powder dissolved to a supersaturation of 40 in 1 h compared to only 22 in the case of a SD. Similar behavior was observed for the highest loading of 16:1, as shown in Figure 5. Even at a lower drug loading commonly used to form SD powders (1:1 ITZ/HPMC), supersaturation of CP particles was 64 in only 20 min compared to only 15 for the SD. As observed for the CP aqueous suspensions, the CP powders dissolved in a few minutes whereas the SD formulations remained as dispersed granules and dissolved on the order of hours. Slow wetting, consistent with the large contact angles, and low surface areas limited the dissolution rate of the SD powders. The small amount of precipitation observed in the

(63) Araya, H.; Nagao, S.; Tomita, M.; Hayashi, M. The Novel Formulation Design of Self-emulsifying Drug Delivery Systems (SEDDS) Type O/W Microemulsion I: Enhancing Effects on Oral Bioavailability of Poorly Water Soluble Compounds in Rats and Beagle Dogs. *Drug Metab. Pharmacokinet.* **2005**, *20* (4), 244–256.

(64) Israelachvili, J. *Intermolecular & Surface Forces*, 2nd ed.; Academic Press: San Diego, 2003.

(65) McCabe, W. L.; Smith, J. C.; Harriott, P. *Unit Operations of Chemical Engineering*, 6th ed.; McGraw-Hill: New York, 2001.

Table 5. Predicted and Experimental Initial Dissolution Rates of Dry Powders (under the conditions used for Figure *6*)

sample	BET area (m^2/g)	total area (A, cm^2)	predicted[a] 10^2 d(m/m_{ltz}^t)/dt (s^{-1})	predicted[b] 10^4 d(m/m_{HPMC}^t)/dt (s^{-1})	experimental[c] 10^4 d(m/m_{ltz}^t)/dt (s^{-1})
1:2 ITZ/HPMC CP	51	27200	22800	91.2	14.6
1:1 ITZ/HPMC CP	23	8100	2560	30.7	10.6
4:1 ITZ/HPMC CP	13	2860	433	6.94	3.54
1:1 ITZ/HPMC solid dispersion	<2	704	1.06	2.67	1.66
4:1 ITZ/HPMC solid dispersion	<2	440	5.06	1.07	1.25

[a] $D_{ITZ} = 4.39 \times 10^{-6}$ cm^2/s from the Wilke–Chang equation;[65] $m_{ltz}{}^t = 17.6$ mg. [b] $k_{HPMC} = 2.67 \times 10^{-5}$ mg cm^{-2} s^{-1}; [67,68] $m_{HPMC}{}^t$ is total mass of HPMC in the dose. [c] Experimental rate based on the sample at 10 min.

case of 1:2 and 1:1 ITZ/HPMC (Figure 6) CP particles after 50 min was likely caused by growth onto the large excess of undissolved drug particles, as the dose was 80. A similar result was observed for dissolution of a nitrindepine SD with HPMC at 14% drug loading.[40]

Table 5 lists the predicted initial dissolution rates for pure ITZ and HPMC, as calculated from eq 1 and the listed values of total surface areas. The first limiting case for the dissolution rate is diffusion of the drug with no inhibition from the HPMC. The second limiting case is dissolution of ITZ governed by the erosion (dissolution) of the HPMC. The ITZ diffusion coefficient was calculated by the Wilke–Chang equation,[65] and the experimental supersaturation value C_{sat} was taken from the maximum levels in Figure 4. For HPMC, a dissolution rate constant (k_{HPMC}) was used from literature[67,68] defined by

$$\frac{dm}{dt} = Ak_{HPMC} \tag{8}$$

where k_{HPMC} is equivalent to $(DC_{sat})/h$ in eq 1 (when $C_t \approx 0$). Experimental initial dissolution rates were estimated from the earliest time point. All of the rates in Table 5 were normalized by the total mass of ITZ or HPMC to convert to a fractional release rate. For amorphous ITZ, experimental values of d(m/m^{tot})/dt were orders of magnitude slower than the calculated values. In contrast, the experimental fractional dissolution rates for ITZ were similar of those of HPMC within the uncertainties in k_{HPMC} and in the measured initial rates. Thus, the polymer dissolution (erosion) appears to be the rate-limiting factor in the overall release of drug for both CP and the lower-surface area SD powders. The much lower mass transfer coefficient for HPMC, 2.67×10^{-5} mg cm^{-2} s^{-1} versus $k_{ITZ} = (D_{ITZ}C_{sat})/h = 1.5 \times 10^{-1}$ to 2.0×10^{-3} mg cm^{-2} s^{-1}, is caused by the slower diffusion coefficient and gelation of HPMC with water. For the CP powders, the HPMC and thus the ITZ dissolution rate increased with a decrease in drug loading as a consequence of the larger surface area. Dissolution rates were typically 1 order of magnitude lower for the SD powders, consistent with the much smaller total surface areas.

Amorphous particles stabilized by HPMC often have slow supersaturation rates in acidic media.[5,36–41] For example, for SD microparticles of ITZ with 67% HPMC loading, the supersaturation reached only ~35 in 1 h.[36] For a more rapidly dissolving polymer, Eudragit E100,[69] supersaturation reached ~73 by 10 min at pH 1.2. However, the drug concentration was unstable (precipitation to ~40 was observed after only 2 h). In both these studies of SD powders, higher loadings were not reported. Typically, at high loadings, such as 80%, drugs in SD such as ITZ[41] may be expected to crystallize, and consequently, the supersaturation values would decrease markedly. However, for CP particles, where amorphous particles are produced at high loadings such as ≥80%, supersaturation values were 63, as shown in Table 4. The high-surface area particles dissolve rapidly to form a supersaturated solution, leaving little time for unwanted crystallization of the solid phase in the presence of solvent. In the case of solid dispersions, sluggish dissolution rates for HPMC allow longer times for the remaining solid phase to crystallize. This effect is particularly evident at high drug loadings, where there is little polymer in the solid phase to protect against solvent-induced crystallization. For SD particles at high drug loadings, such as 4:1 and 16:1 ITZ/HPMC, relatively low supersaturation levels after 4 h of only 40 and 28, respectively, resulted from solid phase crystallization, which was observed in previous studies of amorphous GWX.[57]

4. Conclusions

Controlled precipitation upon mixing of organic solutions and water produced high-surface area amorphous particles, even at drug loadings up to 94%. Excellent wetting and rapid dissolution of the high-surface area amorphous CP particles produced up to 90 times the equilibrium solubility, inhibiting solvent-mediated crystallization of the remaining solid drug in the presence of dissolution media. During controlled precipitation, HPMC partitioned to the water–particle interface, creating a highly wettable polymer-rich surface. Both contact angle measurements and XPS analysis indicated excess hydrophilic HPMC was oriented preferentially on the surface of CP particles. Surface stabilization during CP also

(66) Napper, D. H. *Polymeric Stabilization of Colloidal Dispersions*; Academic Press Inc.: New York, 1983.

(67) Ju, R. T. C.; Nixon, P.; Patel, M. V. Diffusion Coefficients of Polymer Chains in the Diffusion Layer Adjacent to a Swollen Hydrophillic Matrix. *J. Pharm. Sci.* **1997**, *96* (11), 1293–1298.

(68) Siepmann, J.; Kranz, H.; Bodmeier, R.; Peppas, N. A. HPMC-Matrices for Controlled Drug Delivery: A New Model Combining Diffusion, Swelling, and Dissolution Mechanisms and Predicting the Release Kinetics. *Pharm. Res.* **1999**, *16* (11), 1748–1756.

(69) Six, K.; Verreck, G.; Peeters, J.; Brewster, M. E.; Van den Mooter, G. Increased Physical Stability and Improved Dissolution Properties of Itraconazole, a Class II Drug, by Solid Dispersions that Combine Fast- and Slow-Dissolving Polymers. *J. Pharm. Sci.* **2004**, *93* (1), 124–131.

minimized the amount of polymer necessary to arrest growth and quench the drug in the amorphous state. In contrast, for solid dispersions made without water, the level of HPMC was depleted on the surface. ITZ solid dispersions made by solvent evaporation were wetted less effectively by the dissolution media and dissolved slowly, allowing solvent-mediated crystallization of undissolved drug and limiting supersaturation levels to 40 after 4 h. Additionally, ITZ in solid dispersions formed by hot melt extrusion with HPMC crystallizes for drug potencies above 40%.

A thermodynamic analysis indicated that HPMC increased the fugacity of ITZ in the solid phase of CP particles by preventing crystallization of ITZ and by increasing the curvature of the particles and fibers, as described by the Kelvin equation. Whereas HPMC in solution did not affect the supersaturation in the first 4 h, eventually after 24 h, HPMC prevented loss of supersaturation by adsorbing onto embryo crystals smaller than 20 nm to arrest precipitation. The ability to design and produce potent, wettable amorphous nanoparticles for the rapid generation of high levels of supersaturation, with small amounts of hydrophilic stabilizers oriented preferentially at the particle surface, is of significant interest for enhancing the bioavailability of poorly water soluble drugs.

Acknowledgment. We thank Dave Miller for development of the solvent evaporation technique for SD formation, Xiaoxia Gao for assistance with Z-Contrast STEM analysis, and Yangming Sun for XPS analysis. We gratefully acknowledge the financial support from The Dow Chemical Co. (Midland, MI). This material is based upon work supported in part by the STC Program of the National Science Foundation under Agreement CHE-9876674 and the Welch Foundation.

MP0700211